

On the state of sublithospheric upper mantle beneath a supercontinent

Jun Korenaga^{1,*} and Thomas H. Jordan²

¹Department of Earth, Atmospheric, and Planetary Sciences, Massachusetts Institute of Technology, Cambridge, USA. E-mail: korenaga@seismo.berkeley.edu

²Department of Earth Sciences, University of Southern California, Los Angeles, USA

Accepted 2001 October 25. Received 2001 October 17; in original form 2000 November 5

SUMMARY

An assumption of isothermal and static asthenosphere as the normal state of sublithospheric mantle, as commonly employed in studies of terrestrial magmatism, may be physically implausible for a system cooled from above. The growth of an unstable thermal boundary layer at the base of the lithosphere can lead to small-scale convection, so asthenosphere is expected to be usually convecting. A first-order estimate based on the energetics of convection suggests that mantle upwelling rate associated with such small-scale convection is on the order of 10 cm yr^{-1} for asthenospheric viscosity of 10^{18} – 10^{19} Pa s. To investigate the potential role of such sublithospheric convection in anomalous magmatism associated with rifting of the supercontinent Pangaea, a simple upper-mantle convection problem with thick cratonic lithosphere is considered through finite element modelling. Strong three dimensionality is exhibited in our solutions, and the planform of convection is largely affected by the bottom topography of continental lithosphere. Our model also suggests that differential cooling, imposed by a variation in lithospheric lid thickness, may lead to large-scale convection, which brings uncooled, ‘hot’ material from the base of thick lithosphere to shallow asthenosphere. The potential importance of such sublithospheric convection in magmatism during continental rifting is discussed.

Key words: continental margins, hotspots, mantle convection, upper mantle.

1 INTRODUCTION

Continental rifting during the dispersal of the supercontinent Pangaea was often accompanied by massive magmatism as evidenced by the frequent occurrence of flood basalts and thick igneous crust emplaced along a number of rifted margins (White & McKenzie 1989; Holbrook & Kelemen 1993; Coffin & Eldholm 1994). The thickness of igneous crust formed at such volcanic rifted margins is typically 20–30 km (White *et al.* 1987; Mutter & Zehnder 1988; Holbrook *et al.* 1994). Because normal oceanic crust, which most likely results from decompressional melting of passively upwelling mantle with normal potential temperature ($\sim 1300^\circ\text{C}$) (Klein & Langmuir 1987; McKenzie & Bickle 1988; Kinzler & Grove 1992), is only 6–7 km thick (e.g. White *et al.* 1992), the voluminous magmatism implied by several times thicker igneous crust formed during rifting has been commonly attributed to the upwelling of unusually hot mantle originating in a large plume head (White & McKenzie 1989; Richards *et al.* 1989; Hill *et al.* 1992). On the other hand, continents seem to rift at pre-existing weak zones such as cratonic edges (Wilson 1966; Anderson 1994). Mutter *et al.* (1988) proposed that a sharp lateral thermal gradient produced by lithospheric

necking can result in vigorous, small-scale mantle convection, which may account for the observed voluminous rifting magmatism. As Keen & Boutilier (1995) showed, however, such sharp necking is unlikely in the deformation of ductile mantle. Intense lithospheric necking is fundamental for this type of mechanism, as is assumed *a priori* even in the most recent efforts for this type of modelling (Boutilier & Keen 1999; Keen & Boutilier 2000).

Both types of explanations, i.e. plume models and necking models, implicitly assume that the ‘normal’ state of asthenospheric mantle is isothermal and thus static. Anything that cannot be explained by the passive upwelling of mantle with normal potential temperature, therefore, seems to require some special mechanism. Even if asthenospheric mantle was indeed isothermal at some time, however, cooling from above results in the growth of a thermal boundary layer, which may eventually become unstable and lead to sublithospheric, small-scale convection (Foster 1965; Parsons & McKenzie 1978; Buck & Parmentier 1986; Davaille & Jaupart 1994), after which the resultant thermal structure is no longer isothermal. Static and isothermal asthenosphere, therefore, seems to be a rather extreme case, despite the fact that it is commonly assumed to be normal in studies of terrestrial magmatism. If asthenospheric mantle is usually convecting, then, how does this affect our inferences regarding mantle dynamics based on the products of melting? The importance of small-scale convection may be significant, particularly for

*Now at Department of Earth and Planetary Science, University of California, Berkeley, USA.

magmatism during continental rifting. Unlike mid-ocean ridge magmatism, which may be adequately modelled with steady-state, passive mantle upwelling driven by large-scale plate motion (e.g. McKenzie & Bickle 1988), continental rifting is essentially a transient process, in which an initially null surface divergence evolves into finite-rate spreading. The dynamic aspect of pre-existing sublithospheric convection may be important in calculating the amount of melt generated during rifting, because, when the convective upwelling rate exceeds the surface divergence rate, this can produce ‘excess’ magmatism due to rapid mantle fluxing through the melting zone. This type of active mantle upwelling has been proposed to be important in recent studies on continental rifting magmatism (e.g. Kelemen & Holbrook 1995; Korenaga *et al.* 2000).

The rheology of the Earth’s mantle is characterized by strongly temperature-dependent viscosity. Because most of the temperature variation occurs in nearly rigid lithosphere, the energetics of small-scale convection beneath lithosphere (or stagnant-lid convection) can be approximated by that of isoviscous convection (e.g. Solomatov 1995). Based on the boundary layer theory (e.g. Turcotte & Schubert 1982), the velocity scale of such small-scale convection, U , can be expressed as a function of surface heat flux, q , as (Korenaga 2000)

$$U \sim \sqrt{\frac{\alpha \rho_0 g \kappa D^2 q}{8 \mu k}}, \quad (1)$$

where α is thermal expansivity, ρ_0 is a fluid density at some reference temperature, g is gravitational acceleration, κ is the thermal diffusivity, D is the depth extent of convection, μ is fluid viscosity and k is the thermal conductivity. Cellular convection with a unit aspect ratio is assumed in deriving the above scaling law. In this case, the temperature difference across the thermal boundary layer, ΔT_q , is related to the surface heat flux as

$$\Delta T_q \sim \left(\frac{8 \kappa \mu}{\alpha \rho_0 g} \right)^{1/4} \left(\frac{q}{k} \right)^{3/4}. \quad (2)$$

The thickness of the stagnant lid controls heat flux at the top of the convecting domain. Thicker lithosphere can transfer less heat, so the strength of sublithospheric convection is reduced with increasing lid thickness.

Eq. (1) is only conditionally applicable to stagnant-lid convection, because the generation of negative buoyancy for small-scale convection is constrained by temperature-dependent viscosity. The thickness of the cold thermal boundary layer that can participate in convection is limited by a viscosity ratio corresponding to the temperature drop across the unstable boundary layer, and the viscosity ratio is about 3 for marginally stable convection and can be as high as 10 for fully developed convection (Davaille & Jaupart 1993). The temperature dependency of mantle rheology can be modelled by the following Arrhenius law (e.g. Weertman 1970),

$$\mu(T) = \mu_0 \exp\left(\frac{E}{RT} - \frac{E}{RT_0}\right) \quad (3)$$

where E is activation energy, R is the universal gas constant and μ_0 is reference viscosity at temperature T_0 , for which we use the interior temperature of the convecting domain. Denoting $p = \log(\mu_{\max}/\mu_0)$, where μ_{\max} is the highest viscosity in the unstable boundary layer, the maximum temperature drop allowed in the boundary layer may be expressed as,

$$\Delta T_p \sim -\frac{pRT_0^2}{E} \quad (4)$$

when $\Delta T_p \ll T_0$. The velocity scale derived for isoviscous convection (1) can be applied to stagnant-lid convection, if $\Delta T_q < |\Delta T_p|$.

Using values appropriate for the shallow upper mantle, i.e. $\alpha = 3 \times 10^{-5}$, $\rho_0 = 3.3 \times 10^3 \text{ kg m}^{-3}$, $\kappa = 10^{-6} \text{ m}^2 \text{ s}^{-1}$, $k = 3.3 \text{ W m}^{-1} \text{ K}^{-1}$, and $g = 9.8 \text{ m s}^{-2}$, the velocity scale expected for small-scale convection with a depth extent of 150 km is calculated as a function of asthenospheric viscosity, for several values of surface heat flux (Fig. 1a). With the above thermal conductivity and a temperature difference of 1300 K across the rigid lithosphere, heat fluxes of 40–10 mW m^{-2} approximately correspond to lithospheric thicknesses of 100–400 km, respectively. The viscosity of the asthenosphere is probably in a range of 10^{18} – 10^{19} Pa s, based on laboratory studies (Karato & Wu 1993; Hirth & Kohlstedt 1996) and geophysical observations (Pasay 1981; Weins & Stein 1985; Hager & Clayton 1989). Though the depth extent of this weak asthenosphere is not well-known, mantle viscosity is expected to increase with depth because of its non-zero activation volume (e.g. Karato & Wu 1993). Indeed, the mantle transition zone (400–670 km) seems to have a higher viscosity, of 10^{20} – 10^{21} Pa s, and a further increase in viscosity is also indicated for the lower mantle (Hager *et al.* 1985; Hager

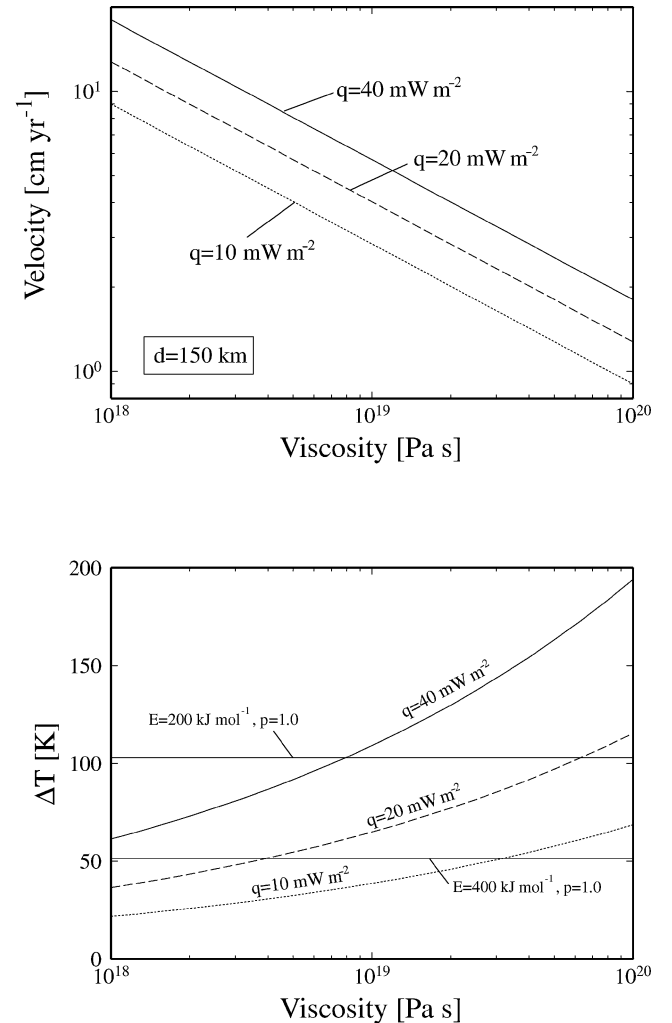


Figure 1. (a) Velocity scale of isoviscous convection subject to a given surface heat flux (eq. 1) is plotted as a function of viscosity. The depth scale of convection is set as 150 km. (b) Temperature drop across cold thermal boundary layer (eq. 2) is compared with the maximum temperature drop imposed by temperature-dependent viscosity (straight lines, eq. 4). The reference temperature T_0 is set as 1573 K. Cases for two values of activation energy (200 and 400 kJ mol^{-1}) and the logarithmic viscosity contrast of 1.0 (corresponding to the viscosity contrasts of 3) are illustrated.

& Clayton 1989; Simons & Hager 1997; Forte & Mitrovica 1996). The depth extent of convection adopted here (150 km) was conservatively chosen in consideration of this likely viscosity layering. For the expected range of asthenospheric viscosity, therefore, small-scale convection beneath 100-km-thick lithosphere may have a velocity scale on the order of 10 cm yr⁻¹, which is an order-of-magnitude higher than a typical rifting rate (~1 cm yr⁻¹). Corresponding temperature variations in the unstable boundary layer are compared with the maximum temperature drop allowed in temperature-dependent mantle rheology (Fig. 1b). Estimates of activation energy for ductile deformation of mantle peridotite vary from 240 kJ mol⁻¹ to 540 kJ mol⁻¹, depending on creep mechanism and the water content in the mantle (Karato & Wu 1993). Though dislocation creep has a higher activation energy (~500 kJ mol⁻¹) than diffusion creep, its large stress exponent (3.0–3.5) can cause a ~50 per cent reduction in the effective activation energy (e.g. Christensen 1984). Indeed, a recent geophysical study of seamount loading suggests activation energy less than 200 kJ mol⁻¹ for oceanic upper mantle (Watts & Zhong 2000). For such low activation energy, the effect of temperature-dependent viscosity on small-scale asthenospheric convection seems to be small (Fig. 1b).

The estimated velocity scale for small-scale convection in the asthenosphere is comparable to or larger than that for typical plate motion. Thus, in the presence of large-scale plate-driven flow, small-scale convection cannot be regarded as a small perturbation, and complex interaction between small-scale convection and plate-driven flow is expected. Our current interest, however, lies in the strength of small-scale convection expected beneath the supercontinent Pangaea. The rifting axes for the Pangaea breakup were located far from subduction zones, so the influence of plate-driven flow is expected to have been minimal for subcontinental mantle. On the other hand, continental lithosphere has a variable thickness because of its long tectonic history, and cratonic lithosphere may be as thick as 300 km (Jordan 1988; Gaherty & Jordan 1995). Because the presence of cratonic lithosphere can reduce convective vigour as well as modulate the pattern of convective planform (Korenaga & Jordan 2001), lateral heterogeneity in lithospheric structure, expected for the amalgamated continental masses (Anderson 1994), has to be incorporated to properly evaluate the velocity field of small-scale convection. The purpose of this paper is, therefore, to explore the possibility of small-scale convection beneath the supercontinent in the pre-rifting period based on numerical modelling, with particular focus on the effect of continental lithosphere, and to quantify the strength and style of pre-existing convection, which may have contributed to rifting magmatism.

2 NUMERICAL FORMULATION

The non-dimensionalized governing equations for thermal convection of an incompressible fluid are:

(i) Conservation of mass

$$\nabla \cdot \mathbf{u} = 0 \quad (5)$$

(ii) Conservation of momentum

$$-\nabla P + \nabla \cdot [\mu(\nabla \mathbf{u} + \nabla \mathbf{u}^T)] - Ra T \mathbf{e}_z = 0 \quad (6)$$

(iii) Conservation of energy

$$\frac{\partial T}{\partial t} + \mathbf{u} \cdot \nabla T = \nabla^2 T + E \quad (7)$$

where P is normalized pressure, E is normalized internal heating, and Ra is the Rayleigh number defined as,

$$Ra = \frac{\alpha \rho_0 g \Delta T d^3}{\kappa \mu_0}, \quad (8)$$

where μ_0 is reference viscosity defined at the top of the system ($z = 1$). The spatial scale is normalized with a system height of d , and the temporal scale is normalized with a diffusion timescale of d^2/κ . Temperature is normalized with ΔT , which is the difference between surface temperature (273 K) and initial asthenospheric temperature (1573 K). To account for possible viscosity layering, we employ temperature- and depth-dependent viscosity as

$$\mu(T, z) = \mu_0(z) \exp\left(\frac{E^*}{T + T_{\text{off}}} - \frac{E^*}{1 + T_{\text{off}}}\right) \quad (9)$$

where $E^* = E/(R\Delta T)$ and $T_{\text{off}} = 273/\Delta T$. The reference viscosity profile, $\mu_0(z)$, is set at 10^{20} for $z = 0$ –0.37 (410–650 km depth), 3×10^{19} for $z = 0.37$ –0.615 (250–410 km depth), and 10^{18} for $z = 0.615$ –1.0 (0–250 km depth). The activation energy is set to 200 kJ mol⁻¹.

The model domain is 650 km deep and 1300 km wide (Fig. 2). A reflecting boundary condition is applied to the side boundaries. The top and bottom boundaries are rigid. The surface temperature is fixed at 273 K, and the bottom boundary is insulated. Normalized internal heat production of 5.0 is uniformly assigned for sublithospheric mantle to approximately compensate surface heat flux. This particular choice of boundary conditions and the use of internal heating may be debatable. When trying to model only a part of the mantle for various reasons, most of the model boundaries are necessarily artificial, and the nature of corresponding boundary conditions is thus somewhat arbitrary. We employed the insulated bottom because we are interested in top-driven convection. Heat flux through the bottom results in the formation of a bottom thermal boundary layer, the dynamics of which can prohibit us from correctly identifying dynamics driven by surface cooling. Because of the insulated bottom boundary, the internal temperature of the system would gradually decrease without internal heating. The upper mantle is generally considered to be depleted in heat-producing elements, and the assumed internal heating to maintain a ‘steady state’ in terms of thermal budget is obviously too high and should be regarded as a compromise coupled with our choice of boundary conditions. We note however, that except for internal temperature, the overall features of model evolution do not significantly differ from the case of no internal heating (Korenaga 2000).

Two sets of model geometry are considered (Fig. 2). In model A, 100-km-thick lithosphere is juxtaposed with a 300-km-thick lithosphere (Fig. 2a). The initial temperature field is prepared by solving steady-state heat conduction subjected to an additional temperature boundary condition of $T = 1573$ K at $z \geq 300$ km (for $0 \leq x < 650$ km) and $z \geq 100$ km (for $x \geq 650$ km). In model B, 200-km-wide and 100-km-thick lithosphere is surrounded by 300-km-thick lithosphere (Fig. 2b), and its initial temperature field is prepared in a similar manner for model A. The velocity of thick lithosphere with initial temperature of less than 1473 K is fixed as zero. The survival of thick cratonic lithosphere (or ‘tectosphere’) for several billion years (e.g. Jordan 1988) requires high activation energy (>500 kJ mol⁻¹) or high intrinsic viscosity (Shapiro & Jordan 1999; Doin *et al.* 1997), so the rheology of continental lithosphere is probably different from that of oceanic mantle. Lenardic & Moresi (1999) suggested that cratonic lithosphere should be intrinsically 10^3 times more viscous than oceanic mantle to account for the longevity of cratonic lithosphere, and this 1000-fold increase is indeed expected

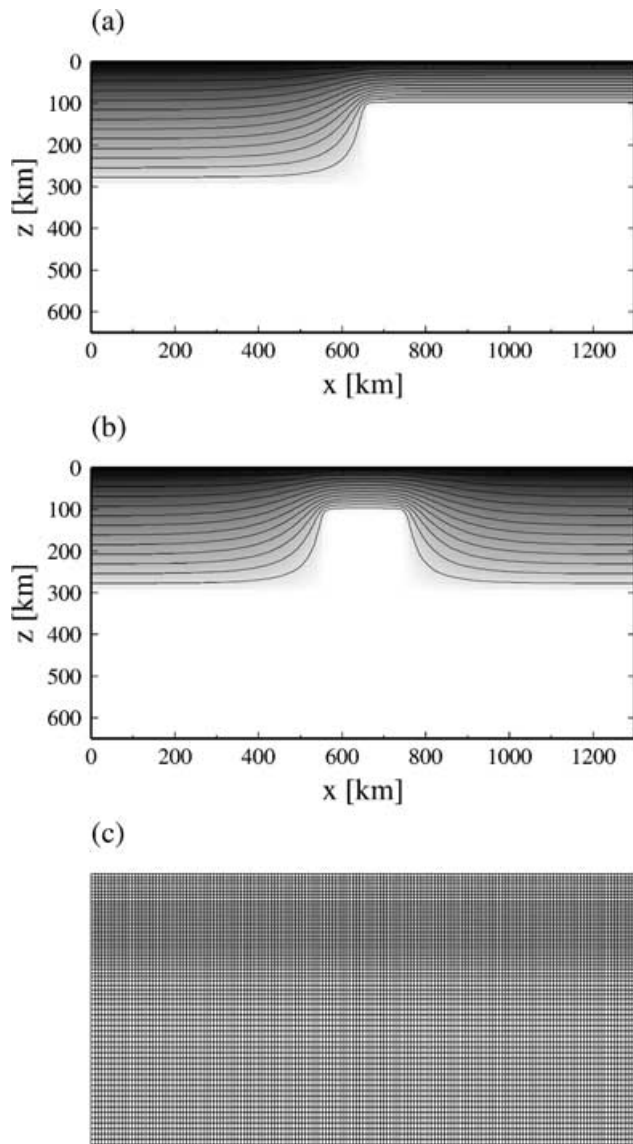


Figure 2. Initial temperature field for finite element modelling. (a) Model A, in which 100-km-thick lithosphere is juxtaposed to 300-km-thick lithosphere. (b) Model B, in which 200-km-wide and 100-km-thick lithosphere is emplaced in 300-km-thick lithosphere. Contours are at 100 K interval. Finite element mesh is shown in (c).

for highly depleted cratonic lithosphere (Jordan 1979; Boyd 1989; Phipps Morgan 1997). Therefore, the assumed rigidity of cratonic lithosphere is probably justified for our modelling of small-scale convection.

The computational domain is discretized with 66×160 variable 2-D quadrilateral elements (Fig. 2c). 2-D numerical solutions to the above coupled differential equations are obtained using the finite element method, the implementation of which is similar to that of ConMan (King *et al.* 1990), except for an optional 3-D single-mode approximation (Korenaga & Jordan 2001). The system is integrated for 200 Myr. The Pangaea supercontinent was formed during the mid-Carboniferous (~ 320 Ma), and its integrity was maintained until the late Jurassic (~ 170 Ma) (Scotese 1984), although incipient rifting events were recorded since the mid-Triassic (Veevers 1989). Thus, the adopted computational period is sufficient to study the dynamics of small-scale convection that might have been present beneath the supercontinent. Because our interest is limited to dy-

namics with a timescale of 100 Myr or so, the rigid bottom boundary may be valid to describe the boundary between the upper and lower mantle. Both viscosity contrast and endothermic phase transition may temporarily hamper material flux through the base of the upper mantle (Tackley *et al.* 1993; Honda *et al.* 1993; Solheim & Peltier 1994; Tackley 1995).

3 RESULTS

The thinnest lithosphere is initially 100-km thick in both types of geometry, so small-scale convection with the velocity scale of ~ 10 cm yr^{-1} is expected beneath the thin spot, based on boundary layer theory (Fig. 1a). Because of the presence of thick continental lithosphere, the temporal evolution of sublithospheric convection is found to be more complex than simple small-scale convection. In the following, we will show some representative snapshots of model evolution and discuss them in detail. We start with the description of 2-D solutions, before presenting more natural, but also relatively more complicated 3-D single-mode solutions.

3.1 2-D solutions

The evolution of model A is shown in Fig. 3. The maximum upwelling and downwelling velocities are measured for asthenospheric mantle in the vicinity of cratonic lithosphere ($z > 400$ km and $325 < x < 975$ km). The largest peak in the maximum downwelling velocity (Fig. 3e) observed at ~ 5 Myr corresponds to the formation of the first cold downwelling from the base of thin lithosphere. This onset of instability excites small-scale convection, and the maximum upwelling velocity fluctuates around 5–10 cm yr^{-1} during the first 40 Myr. Due to the viscosity increase with depth, this convection is almost confined to the asthenosphere (Fig. 3a). There is persistent, weaker downwelling along the cratonic side wall, but during the first 40 Myr, there is no indication that small-scale convection is modulated by cratonic lithosphere. Upwellings are mainly controlled by downwellings from the base of thin lithosphere, and they migrate through time. This is because the lateral temperature gradient within the cratonic lithosphere is smaller than the vertical temperature gradient in the thin lithosphere. The generation of negative buoyancy due to side wall cooling is not large enough to compete with random downwellings beneath the thin lithosphere. Upwelling is slower and more diffuse than downwelling, because the former occurs in response to focused downwelling.

However, after the first 40 Myr or so, the emergence of another convective pattern is observed. The maximum upwelling velocity becomes comparable with the maximum downwelling velocity (Fig. 3e). This corresponds to strong upwelling from the base of the cratonic lithosphere to shallow asthenosphere, and this seems to suppress the formation of random downwelling from the thin lithosphere (Figs 3c and d). Though downwelling along the cratonic side wall is still present, which tends to deflect this upwelling (Figs 3b–d), the location of upwelling is persistent through time. This stable, larger-scale convection results from differential cooling imposed by the variation in lithosphere thickness. Whereas the vigorous small-scale convection efficiently cools the asthenosphere beneath the thin lithosphere, the mantle beneath the cratonic lithosphere is relatively uncooled. This leads to the development of a large-scale lateral temperature gradient in the sublithospheric mantle, by which relatively hot, deep mantle flows to shallower depths. This large-scale flow is conceptually similar to a mechanism advocated by King & Anderson (1995, 1998) for the generation of continental flood basalts.

Results with model B are in general similar to those with model A, except that stronger effects of side walls are observed (Fig. 4).

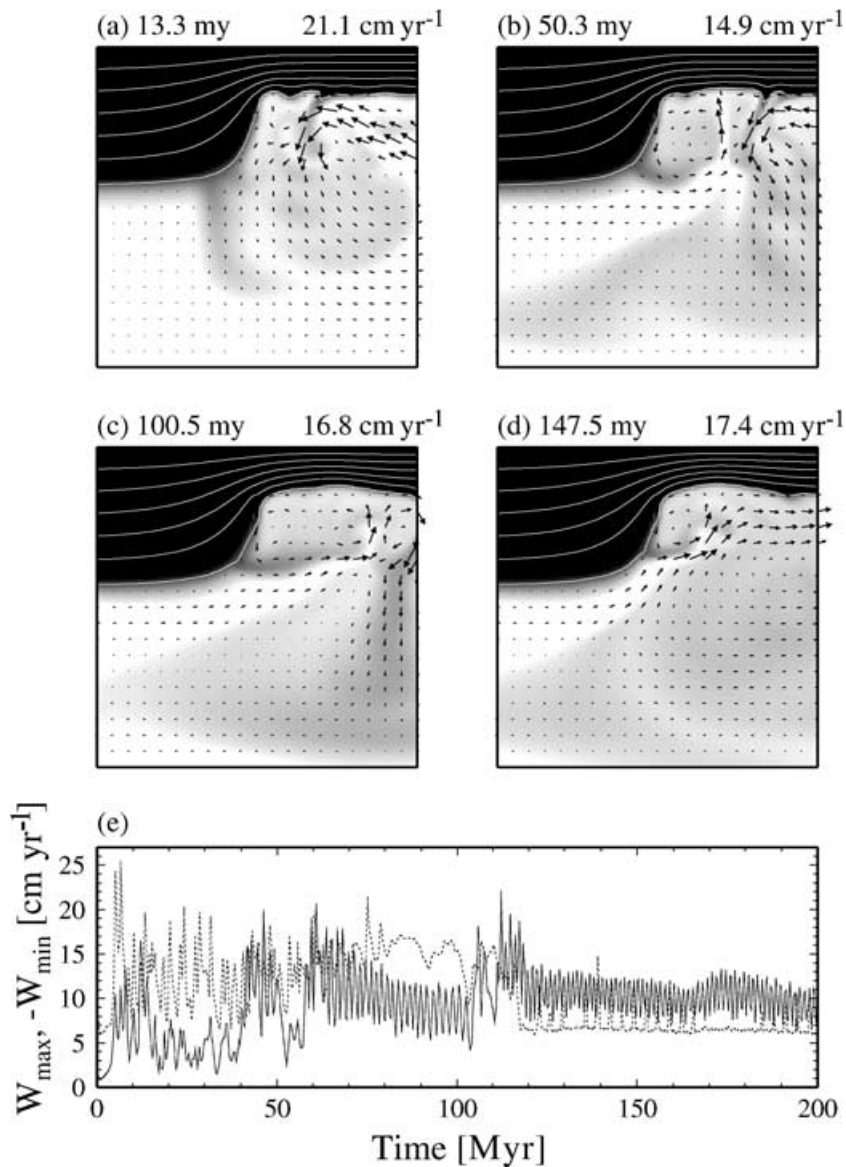


Figure 3. 2-D evolution of model A. Snapshots are shown in (a)–(d). Maximum velocity is shown on the top-right for each snapshot. Contour interval is 200 K. Note that temperature shading is different from Fig. 2 to present subtle variation associated with small-scale convection. The time-series of maximum upwelling velocity (solid) and maximum downwelling velocity (dash) are shown in (e).

Except for the very first downwelling, the strengths of upwelling and downwelling are comparable during the early model evolution (Fig. 4e). This is simply the geometric effect of the lithospheric lid. Because of the closely spaced cratonic side walls, the pattern of small-scale convection is fixed. Return flow to downwellings along side walls takes place as focused upwellings into the thin spot (Fig. 4a). The effect of differential surface cooling is also observed after the first 60 Myr; a broad cold downwelling from the centre of the thin spot brings uncooled mantle beneath the cratonic lithosphere into the thin spot (Figs 4c and d). Unlike in model A, however, there are two large-scale upwellings trying to flow into the thin spot from both sides. Competition between them results in the oscillatory nature of the maximum upwelling velocity (Fig. 4e).

3.2 3-D single-mode solutions

The analysis of the convective instability of an isoviscous fluid in the presence of conducting side wall suggests that the preferred

planform of convection is always 3-D, in which convection cells are aligned perpendicular to a side wall (Korenaga & Jordan 2001). The velocity reduction due to side walls is also expected to be mitigated in 3-D convection. To explore this potential importance of 3-D convection in our model with variable viscosity, we computed 3-D single-mode solutions using the method developed by Korenaga & Jordan (2001). In this approximation, any variation in the out-of-plane coordinate (i.e. the horizontal coordinate parallel to side walls), y , has only one mode with a particular wavenumber, ψ . For example, a temperature field is described as

$$T(x, y, z) = T(x, z) + \theta(x, z) \cos(\psi y), \quad (10)$$

where $T(x, z)$ and $\theta(x, z)$ are called basic-field temperature and deviation temperature, respectively. Similar nomenclature is used for other variables such as pressure and velocity.

This approximation essentially reduces a 3-D problem to a 2-D one, and it is only about twice as expensive both in computation time and memory usage, compared with a purely 2-D calculation.

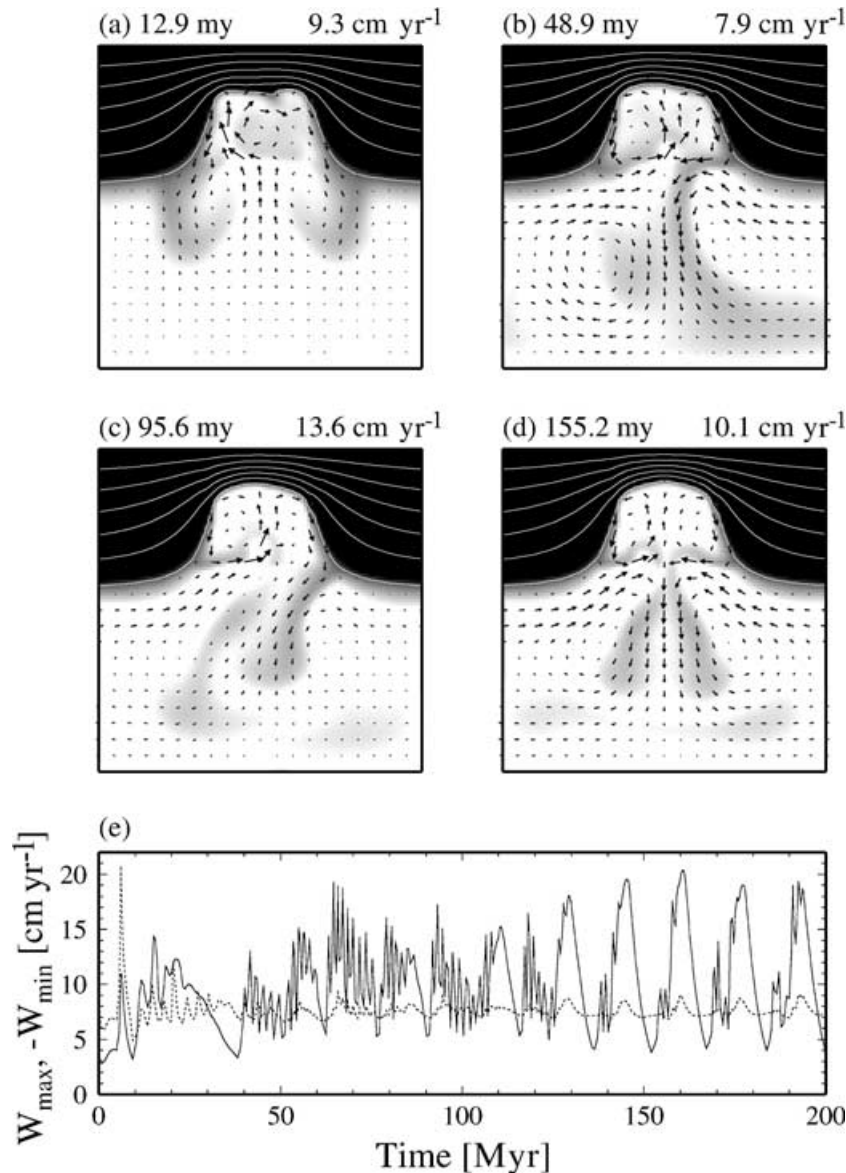


Figure 4. 2-D evolution of model B. Time-series and snapshots are shown in the same manner of Fig. 3.

Representing out-of-plane variation by only one mode may be a crude approximation, but it suffices our primary purpose here, which is to observe whether or not 3-D convection is excited at all. Model parameters are identical to those used for 2-D solutions. The initial deviation temperature field has random perturbations with an amplitude of 0.1 K. The out-of-plane wavenumber is set as 2π given the expected spatial scale of convection. In addition to velocity statistics, basic-field kinetic energy and deviation kinetic energy are calculated from corresponding velocity fields; the ratio of deviation kinetic energy to total kinetic energy (i.e. basic field plus deviation) quantifies the three dimensionality of convection. We note that the 3-D single-mode approximation tends to underestimate the strength of the out-of-plane convection (Korenaga & Jordan 2001), so deviation kinetic energy in a fully 3-D solution would be larger than that in a single-mode solution.

Fig. 5 shows the evolution of model A, which is in general similar to its 2-D version. It is characterized first by small-scale convection beneath the thin lithosphere (Fig. 5a), and then the differential cooling effect eventually generates larger-scale convection (Figs 5b

and c). The mode of out-of-plane convection is excited at ~ 5 Myr, which coincides with the formation of the first downwelling (Fig. 5d). The contribution of deviation kinetic energy to total kinetic energy rapidly increases in the next 15 Myr until its proportion reaches ~ 0.7 . The average proportion is ~ 0.5 in the first 100 Myr, and it gradually decreases to 0.2–0.1 in the next 100 Myr. This reduced three dimensionality may imply that either (1) the planform of large-scale convection in the later phase is not properly handled by the prescribed out-of-plane wavenumber, which is optimal for small-scale convection in asthenosphere, or (2) three dimensionality is not important for the large-scale convection, for which the effect of cratonic side wall is probably small. The maximum upwelling velocity is consistently ~ 50 per cent higher than that of the 2-D solution, and its average value is ~ 15 cm yr $^{-1}$ (Fig. 5d).

A similar enhancement of convection is also observed for model B (Fig. 6). As in the 2-D case, downwellings along side walls tend to focus upwelling into the thin spot. The excitation of out-of-plane convection follows this pattern of convection modulated by side

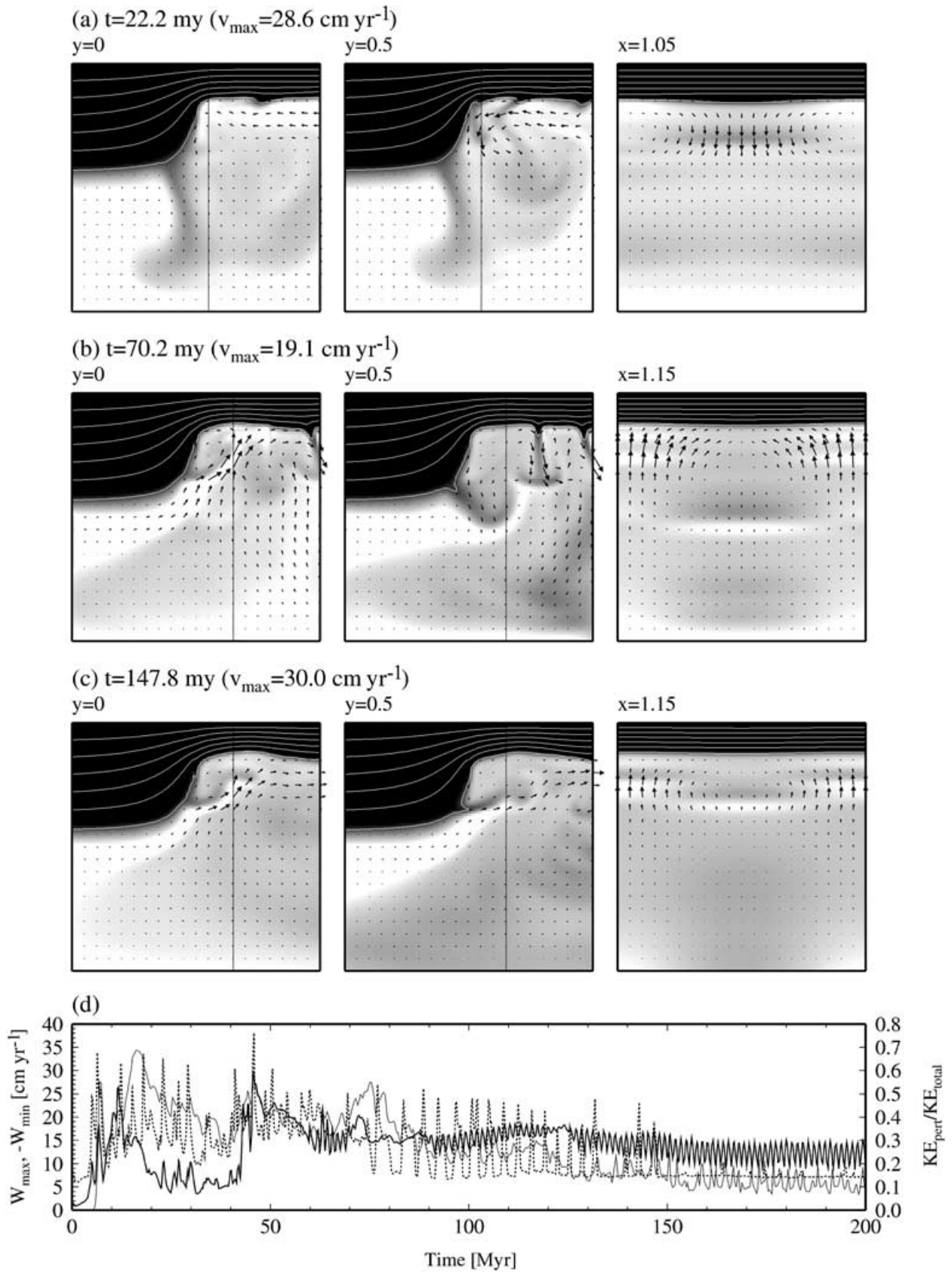


Figure 5. 3-D single-mode solution for model A. Snapshots are shown in (a)–(c). Three cross-sections are shown for each snapshot, with the planes of $y = 0$, $y = 0.5$, and $x = \text{constant}$. This constant is chosen snapshot to snapshot to highlight the three dimensionality (or lack thereof) of convection. The time series of maximum upwelling velocity (thick solid), maximum downwelling velocity (thick dash), and the ratio of deviation kinetic energy to total kinetic energy (thin solid) are shown in (d).

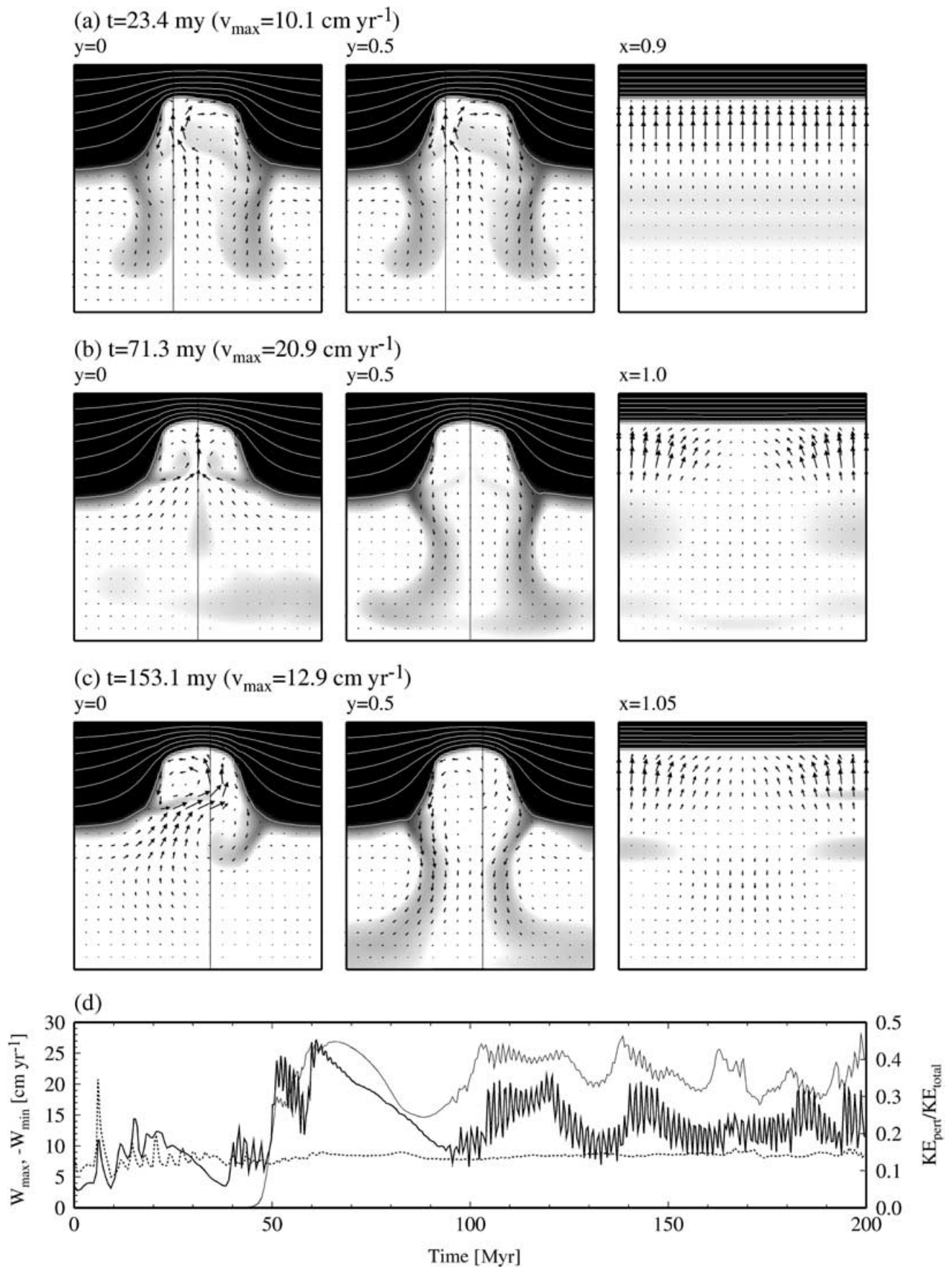


Figure 6. Same as Fig. 5, but for model B.

walls, as expected from the fact that the deviation temperature field must share the same type of symmetry with the 2-D basic-field temperature field (Korenaga & Jordan 2001). It is interesting to note that three-dimensional convection is not observed for the first 50 Myr (Figs 6a and d). The preference of a 3-D convective planform in a fluid bounded by side walls, as suggested by Korenaga & Jordan (2001), is only for stationary state convection, and this example indicates that it does not apply to the early stage of transient convection.

4 DISCUSSION AND CONCLUSION

As a preliminary attempt to explore the possibility of sublithospheric convection beneath a supercontinent, several important complications pertinent to the Earth's mantle have been left for future work, such as non-Newtonian rheology and more realistic bottom boundary conditions. Because the dynamic origin of small-scale convection is the instability of a top thermal boundary layer, and because the strength of convection is sensitive to the portion of the boundary layer that can be detached, the role of stress-dependent viscosity in destabilizing the boundary layer is probably important for finite-amplitude convection (e.g. Schmeling & Marquart 1993; Solomatov 1995; Schmeling & Bussod 1996; Larsen & Yuen 1997). We used the insulating bottom boundary to isolate the dynamics originated in cooling from the above. In the real mantle, however, we expect some form of heat transfer from the lower mantle. Because the actual realization of such transfer may be highly case-dependent, we regard the choice of some particular form of heat flux as unwarranted. The dynamics of small-scale convection would be inevitably affected by such heat flux from below, and our study with the insulating bottom boundary should be regarded as a limiting case.

The viscosity law used in our model incorporates (1) temperature dependency with relatively low activation energy as inferred by a recent geodynamic study, (2) depth dependency expected from non-zero activation volume and also possibly from phase changes, and (3) intrinsic variation associated with probable chemical heterogeneity within lithosphere (i.e. the rigidity of thick cratonic tectosphere). In addition to the model runs presented in the previous section, we have conducted a number of sensitivity tests by varying activation energy and so on (e.g. Korenaga 2000), and we found that all of the above features are important for the generation of steadily strong sublithospheric convection. Increasing activation energy leads to more sluggish convection; the activation energy of 400 kJ mol^{-1} reduces the maximum upwelling velocity by ~ 50 per cent. Depth-dependent viscosity and the structural stability of heterogeneous continental lithosphere are both important for the generation of the 'differential cooling' mode. Small-scale convection tends to be confined in shallow depths by depth-dependent viscosity, which prevents horizontal mixing in sublithospheric mantle. If cratonic tectosphere is not strong enough, its relatively high local Rayleigh number would destabilize it in a relatively short timescale (Jordan 1988; Shapiro & Jordan 1999). Intrinsic rheological heterogeneity must be important as well as intrinsic chemical heterogeneity. We would like to emphasize that, however, even if these conditions are met, the differential cooling mode is not always guaranteed (e.g. Fig. 6). How small-scale convection is generated and evolves in response to a given lithospheric structure is a delicate matter that is very sensitive to an adopted viscosity law, and it is usually difficult to confidently draw some specific conclusions on the expected geometry of convective flow based on a limited number of model runs, though this point tends to be overlooked (e.g. King & Ritsema 2000).

To apply the idea of strong sublithospheric convection to rifting magmatism, it will be necessary to consider how rifting affects this pre-existing convection. Because small-scale convection is driven by negative buoyancy, the strength of upwellings probably remains similar as long as the distribution of negative buoyancy is not severely destroyed by rapid rifting. As rifting proceeds and evolves into seafloor spreading, mantle flow will be eventually dominated by plate-driven flow, and it may be important to investigate the timescale of this transition as well as the temporal variation in the planform of convection. Mantle melting may add further complication to the dynamics of small-scale convection (e.g. Tackley & Stevenson 1993).

The purpose of this paper is not to challenge the importance of plumes in mantle dynamics. A number of numerical studies of whole-mantle convection show that plumes are the most preferred style of upwelling. Our intention is simply to point out that 'normal' asthenosphere can exhibit the rich dynamics of small-scale convection. A currently prevailing tendency in studies of large igneous provinces is that anything that cannot be explained by the passive upwelling of normal asthenosphere is regarded as the influence of a mantle plume. We have shown that, using an acceptable range of rheological parameters for the Earth's upper mantle, vigorous upwelling in asthenosphere is a likely state of sublithospheric mantle. A variation in the thickness of continental lithosphere can modulate the pattern of convection, and as a result, upwelling tends to be focused toward a thinner spot, which is also a potential locus for rifting. Even when the overlying lithospheric structure is pre-dominantly 2-D, 3-D convection is the fundamental character of sublithospheric convection, which may evolve into focused upwelling on a rifting axis. The formation of large-scale thermal structure and corresponding convection in sublithospheric mantle is also likely when the thickness variation of lithosphere results in differential cooling. Because the upper mantle is not expected to be isothermal in the first place, due to various kinds of previous tectonic history (e.g. Anderson *et al.* 1992), the strength of small-scale convection and the temperature of convecting region may also be influenced by pre-existing thermal anomalies. When we are to investigate the origin of some 'anomalous' magmatism, therefore, it may be worth first questioning what could happen without mantle plumes.

ACKNOWLEDGMENTS

This work was sponsored by the U.S. National Science Foundation under grant EAR-0049044. We thank Jack Whitehead, Brad Hager, Maria Zuber, Peter Kelemen, Steve Holbrook, and Bob Detrick for constructive comments on the earlier version of this manuscript. Critical reviews by Harro Schmeling and Betram Schott were also very helpful.

REFERENCES

- Anderson, D.L., 1994. Superplumes or supercontinents?, *Geology*, **22**, 39–42.
- Anderson, D.L., Tanimoto, T. & Zhang, Y.S., 1992. Plate tectonics and hotspots; the third dimension, *Science*, **256**, 1645–1651.
- Boutillier, R.R. & Keen, C.E., 1999. Small-scale convection and divergent plate boundaries, *J. geophys. Res.*, **104**, 7389–7403.
- Boyd, F.R., 1989. Compositional distinction between oceanic and cratonic lithosphere, *Earth planet. Sci. Lett.*, **96**, 15–26.
- Buck, W.R. & Parmentier, E.M., 1986. Convection beneath young oceanic lithosphere: Implications for thermal structure and gravity, *J. geophys. Res.*, **91**, 1961–1974.

- Christensen, U., 1984. Convection with pressure- and temperature-dependent non-Newtonian rheology, *Geophys. J. R. astr. Soc.*, **77**, 343–384.
- Coffin, M.F. & Eldholm, O., 1994. Large igneous provinces: Crustal structure, dimensions, and external consequences, *Rev. Geophys.*, **32**, 1–36.
- Davaille, A. & Jaupart, C., 1993. Transient high-Rayleigh-number thermal convection with large viscosity variations, *J. Fluid Mech.*, **253**, 141–166.
- Davaille, A. & Jaupart, C., 1994. Onset of thermal convection in fluids with temperature-dependent viscosity: Application to the oceanic mantle, *J. geophys. Res.*, **99**, 19 853–19 866.
- Doin, M.-P., Freitout, L. & Christensen, U., 1997. Mantle convection and stability of depleted and undepleted continental lithosphere, *J. geophys. Res.*, **102**, 2771–2787.
- Forté, A.M. & Mitrovica, J.X., 1996. New inferences of mantle viscosity from joint inversion of long-wavelength mantle convection and post-glacial rebound data, *Geophys. Res. Lett.*, **23**, 1147–1150.
- Foster, T.D., 1965. Stability of a homogeneous fluid cooled uniformly from above, *Phys. Fluids*, **8**, 1249–1257.
- Gaherty, J.B. & Jordan, T.H., 1995. Lehmann discontinuity as the base of an anisotropic layer beneath continents, *Science*, **268**, 1468–1471.
- Hager, B.H. & Clayton, R.W., 1989. Constraints on the structure of mantle convection using seismic observations, flow models, and the geoid, in *Mantle Convection and Global Dynamics*, pp. 657–763, ed. Peltier, W.R., Gordon and Breach Science Publishers. New York.
- Hager, B.H., Clayton, R.W., Richards, M.A., Comer, R.P. & Dziewonski, A.M., 1985. Lower mantle heterogeneity, dynamic topography and the geoid, *Nature*, **313**, 541–545.
- Hill, R.I., Campbell, I.H., Davies, G.F. & Griffiths, R.W., 1992. Mantle plumes and continental tectonics, *Science*, **256**, 186–193.
- Hirth, G. & Kohlstedt, D.L., 1996. Water in the oceanic mantle: Implications for rheology, melt extraction, and the evolution of the lithosphere, *Earth planet. Sci. Lett.*, **144**, 93–108.
- Holbrook, W.S. & Kelemen, P.B., 1993. Large igneous province on the US Atlantic margin and implications for magmatism during continental breakup, *Nature*, **364**, 433–436.
- Holbrook, W.S., Reiter, E.C., Purdy, G.M., Sawyer, D., Stoffa, P.L., Austin, J.A.J., Oh, J. & Makris, J., 1994. Deep structure of the U.S. Atlantic continental margin, offshore south carolina, from coincident ocean bottom and multichannel seismic data, *J. geophys. Res.*, **99**, 9155–9178.
- Honda, S., Yuen, D.A., Balachandrar, S. & Reuteler, D., 1993. Three-dimensional instabilities of mantle convection with multiple phase transitions, *Science*, **259**, 1308–1311.
- Jordan, T.H., 1979. Mineralogies, densities and seismic velocities of garnet lherzolites and their geophysical implications, in *The Mantle Sample: Inclusions in Kimberlites and Other Volcanics*, pp. 1–14, Boyd, F.R. & Meyer, H.D.A., eds, American Geophysical Union, Washington DC.
- Jordan, T.H., 1988. Structure and formation of the continental tectosphere, *J. Petrol. Spec.*, 11–37.
- Karato, S. & Wu, P., 1993. Rheology of the upper mantle: A synthesis, *Science*, **260**, 771–778.
- Keen, C.E. & Boutilier, R.R., 1995. Lithosphere-asthenosphere interactions below rifts, in *Rifted Ocean-Continent Boundaries*, Banda, E., Talwan, M. & Torne, M., eds, pp. 17–30, Kluwer, Boston.
- Keen, C.E. & Boutilier, R.R., 2000. Interaction of rifting and hot horizontal plume sheets at volcanic margins, *J. geophys. Res.*, **105**, 13 375–13 387.
- Kelemen, P.B. & Holbrook, W.S., 1995. Origin of thick, high-velocity igneous crust along the U.S. East Coast Margin, *J. geophys. Res.*, **100**, 10 077–10 094.
- King, S.D. & Anderson, D.L., 1995. An alternative mechanism of flood basalt formation, *Earth planet. Sci. Lett.*, **136**, 269–279.
- King, S.D. & Anderson, D.L., 1998. Edge-driven convection, *Earth planet. Sci. Lett.*, **160**, 289–296.
- King, S.D. & Ritsema, J., 2000. African hot spot volcanism: small-scale convection in the upper mantle beneath cratons, *Science*, **290**, 1137–1140.
- King, S.D., Raefsky, A. & Hager, B.H., 1990. ConMan: vectorizing a finite element code for incompressible two-dimensional convection in the earth's mantle, *Phys. Earth planet. Inter.*, **59**, 195–207.
- Kinzler, R.J. & Grove, T.L., 1992. Primary magmas of mid-ocean ridge basalts, 2, applications, *J. geophys. Res.*, **97**, 6907–6926.
- Klein, E.M. & Langmuir, C.H., 1987. Global correlations of ocean ridge basalt chemistry with axial depth and crustal thickness, *J. geophys. Res.*, **92**, 8089–8115.
- Korenaga, J., 2000. Magmatism and Dynamics of Continental Breakup in the Presence of a Mantle Plume, *PhD thesis*, MIT/WHOI Joint Program, Cambridge, MA.
- Korenaga, J. & Jordan, T.H., 2001. Effects of vertical boundaries on infinite prandtl number thermal convection, *Geophys. J. Int.*, **147**, 639–659.
- Korenaga, J., Holbrook, W.S., Kent, G.M., Kelemen, P.B., Detrick, R.S., Larsen, H., Hopper, J.R. & Dahl-Jensen, T., 2000. Crustal structure of the southeast Greenland margin from joint refraction and reflection seismic tomography, *J. geophys. Res.*, **105**, 21 591–21 614.
- Larsen, T.B. & Yuen, D.A., 1997. Fast plumeheads: Temperature-dependent versus non-newtonian rheology, *Geophys. Res. Lett.*, **24**, 1995–1998.
- Lenardic, A. & Moresi, L.-N., 1999. Some thoughts on the stability of cratonic lithosphere: Effects of buoyancy and viscosity, *J. geophys. Res.*, **104**, 12 747–12 758.
- McKenzie, D. & Bickle, M.J., 1988. The volume and composition of melt generated by extension of the lithosphere, *J. Petrol.*, **29**, 625–679.
- Mutter, J.C. & Zehnder, C.M., 1988. Deep crustal structure and magmatic processes: The inception of seafloor spreading in the norwegian-greenland sea, in *Early Tertiary Volcanism and the Opening of the NE Atlantic*, Vol. 39, pp. 35–48, eds Morton, A.C. & Parson, L.M., Geological Society of London, London.
- Mutter, J.C., Buck, W.R. & Zehnder, C.M., 1988. Convective partial melting, 1, a model for the formation of thick basaltic sequences during the initiation of spreading, *J. geophys. Res.*, **93**, 1031–1048.
- Parsons, B. & McKenzie, D., 1978. Mantle convection and the thermal structure of the plates, *J. geophys. Res.*, **83**, 4485–4496.
- Pasay, Q.R., 1981. Upper mantle viscosity derived from the difference in rebound of the Provo and Bonneville shorelines: Lake bonneville basin, Utah, *J. geophys. Res.*, **86**, 11 701–11 708.
- Phipps Morgan, J., 1997. The generation of a compositional lithosphere by mid-ocean ridge melting and its effect on subsequent off-axis hotspot upwelling and melting, *Earth planet. Sci. Lett.*, **146**, 213–232.
- Richards, M.A., Duncan, R.A. & Courtillot, V.E., 1989. Flood basalts and hot-spot tracks: Plume heads and tails, *Science*, **246**, 103–107.
- Schmeling, H. & Bussod, G.Y., 1996. Variable viscosity convection and partial melting in the continental asthenosphere, *J. geophys. Res.*, **101**, 5411–5423.
- Schmeling, H. & Marquart, G., 1993. Mantle flow and the evolution of the lithosphere, *Phys. Earth planet. Int.*, **79**, 241–267.
- Scotese, C.R., 1984. *Paleomagnetism and the Assembly of Pangaea*, American Geophysical Union, Washington DC.
- Shapiro, S.S. & Jordan, T.H., 1999. Stability and dynamics of the continental tectosphere, *Lithos*, **48**, 115–133.
- Simons, M. & Hager, B.H., 1997. Localization of the gravity field and the signature of glacial rebound, *Nature*, **390**, 500–504.
- Solheim, L.P. & Peltier, W.R., 1994. Avalanche effects in phase transition modulated thermal convection, *J. geophys. Res.*, **99**, 6997–7018.
- Solomatov, V.S., 1995. Scaling of temperature- and stress-dependent viscosity convection, *Phys. Fluids*, **7**, 266–274.
- Tackley, P.J., 1995. On the penetration of an endothermic phase transition by upwellings and downwellings, *J. geophys. Res.*, **100**, 15 477–15 488.
- Tackley, P.J. & Stevenson, D., 1993. A mechanism for spontaneous self-perpetuating volcanism on the terrestrial planets, in *Flow and Creep in the Solar System: Observations, Modeling and Theory*, pp. 307–321, eds Stone, D.B. & Runcorn, S.K., Kluwer Academic, Boston.
- Tackley, P.J., Stevenson, D.J., Glatzmaier, G.A. & Schubert, G., 1993. Effects of an endothermic phase transition at 670 km depth in a spherical model of convection in the earth's mantle, *Nature*, **361**, 699–704.
- Turcotte, D.L. & Schubert, G., 1982. *Geodynamics: Applications of continuum physics to geological problems*, John Wiley & Sons, New York.
- Veevers, J.J., 1989. Middle-late Triassic (230 + 5 Ma) singularity in the stratigraphic and magmatic history of the Pangean heat anomaly, *Geology*, **17**, 784–787.
- Watts, A.B. & Zhong, S., 2000. Observations of flexure and the rheology of oceanic lithosphere, *Geophys. J. Int.*, **142**, 855–875.

- Weertman, J., 1970. The creep strength of the Earth's mantle, *Rev. Geophys. Space Phys.*, **8**, 146–168.
- Weins, D.A. & Stein, S., 1985. Implications of oceanic intraplate seismicity for plate stresses, driving forces and rheology, *Tectonophysics*, **116**, 143–162.
- White, R. & McKenzie, D., 1989. Magmatism at rift zones: The generation of volcanic continental margins and flood basalts, *J. geophys. Res.*, **94**, 7685–7729.
- White, R.S., Spence, G.D., Fowler, S.R., McKenzie, D.P., Westbrook, G.K. & Bowen, A.N., 1987. Magmatism at rifted continental margins, *Nature*, **330**, 439–444.
- White, R.S., McKenzie, D. & O'Nions, R.K., 1992. Oceanic crustal thickness from seismic measurements and rare earth element inversions, *J. geophys. Res.*, **97**, 19 683–19 715.
- Wilson, J.T., 1966. Did the Atlantic close and then re-open?, *Nature*, **211**, 676–681.